Modeling the influence of open water surfaces on the summertime temperature and thermal comfort in the city

Article

Published Version

JOURNAL OF GEOPHYSICAL RESEARCH: ATMOSPHERES, VOL. 118, 8881–8896, doi:10.1002/jgrd.50704, 2013

Modeling the influence of open water surfaces on the summertime temperature and thermal comfort in the city

N. E. Theeuwes,[1] A. Solcerová,[1] and G. J. Steeneveld[1]

Received 3 April 2013; revised 27 June 2013; accepted 30 July 2013; published 26 August 2013.

[1] Due to the combination of rapid global urbanization and climate change, urban climate issues are becoming relatively more important and are gaining interest. Compared to rural areas, the temperature in cities is higher (the urban heat island effect) due to the modifications in the surface radiation and energy balances. This study hypothesizes that the urban heat island can be mitigated by introducing open surface water in urban design. In order to test this, we use the WRF mesoscale meteorological model in which an idealized circular city is designed. Herein, the surface water cover, its size, spatial configuration, and temperature are varied. Model results indicate that the cooling effect of water bodies depends nonlinearly on the fractional water cover, size, and distribution of individual lakes within the city with respect to wind direction. Relatively large lakes show a high temperature effect close to their edges and in downwind areas. Several smaller lakes equally distributed within the urban area have a smaller temperature effect, but influence a larger area of the city. Evaporation from open water bodies may lower the temperature, but on the other hand also increases the humidity, which dampens the positive effect on thermal comfort. In addition, when the water is warmer than the air temperature (during autumn or night), the water body has an adverse effect on thermal comfort. In those cases, the water body eventually limits the cooling and thermal comfort in the surrounding city, and thus diverges from the original intention of the intervention.

Citation: Theeuwes, N. E., A. Solcerová, and G. J. Steeneveld (2013), Modeling the influence of open water surfaces on the summertime temperature and thermal comfort in the city, *J. Geophys. Res. Atmos.*, *118*, 8881–8896, doi:10.1002/jgrd.50704.

1. Introduction

[2] In the last century, the percentage of people living in cities increased from 13% in 1900 to 49% in 2005 [*United Nations*, 2005]. This number is projected to increase even further in coming years and decades. A second important aspect for the urban environment is the projected climate change [*McCarthy et al.*, 2010]. In a changing climate, the number of heat waves is expected to increase in the next century, e.g., up to a factor of nine for Chicago [*Peng et al.*, 2011]. This has aggravated effects on the urban area [*Tan et al.*, 2010], and the added pressure on cities shows the importance and urgency of understanding the physics of the urban climate.

[3] One of the key aspects of the urban climate is the higher nocturnal temperature in cities compared to the rural surroundings. This phenomenon is known as the urban heat island (UHI) and may cause severe discomfort to inhabitants, especially during hot summer days and nights [*Patz et al.*, 2005; *Vandentorren et al.*, 2006, *Tomlinson et al.*, 2011]. This research focuses on the evolution of the urban temperature during a full diurnal cycle (24 h) and studies the effectiveness of water bodies in the city as intervention tools, for both day and night. We assess the instantaneous air temperature at the 2 m level and quantify the modeled urban temperature with and without intervention using lakes.

[4] The main objective of this work is to quantitatively investigate the influence of the water bodies on the urban temperature and human thermal comfort. This objective is divided into four separate subtopics. First, we study how the spatial distribution of water bodies and water fraction in the city influences the temperature in the urban area. Second, we quantify the influence of the lake water temperature on the urban temperature. The third topic covers the technical aspect of the model, i.e., how the selected atmospheric boundary layer (ABL) schemes can influence the results. The final topic is a quantification of the results for thermal comfort.

[5] This research is not based on field measurements, but approaches the objectives with a mesoscale meteorological model. In this way, we are able to study a city with an idealized setup, which allows us to draw general conclusions rather than conclusions for a specific city. Experiments in which lakes can be modified are virtually impossible in practice. In addition, field observations around different water bodies are not representative of only the studied feature (in our case, it would be the presence of an open water body), but are also influenced by several other aspects like orography or land use. These issues can be easily solved in a model environment by changing the spatial characteristics of the city and its surrounding rural areas. We used this possibility to create a circular city and study the temperature change

[1]Meteorology and Air Quality Section, Wageningen University, Wageningen, Netherlands.

Corresponding author: N. E. Theeuwes, Meteorology and Air Quality Section, Wageningen University, PO box 47, Wageningen, NL-6700 AA, Netherlands. (Natalie.Theeuwes@wur.nl)

2169-897X/13/10.1002/jgrd.50704

under influence of different size and distribution of water bodies within the urban area.

[6] This paper is organized as follows. Section 2 gives a theoretical background of the problem and reviews the literature related to the topic. Section 3 describes the used methods and different approaches to assess the influence of water bodies on the urban temperature. Section 4 describes the results connected to the different approaches, followed by a short assessment of the influence on human thermal comfort. Finally, we discuss the results in section 5 and give some conclusions in section 6.

2. Theoretical Background

[7] The UHI, here defined as the air temperature difference between a rural grass field and the urban canopy layer temperature [*Stewart and Oke*, 2012], is mainly caused by a different energy balance in cities compared to rural areas,

$$Q^* + ANT = SH + LH + G \quad (1)$$

where Q^* is the net radiation ($\mathrm{Wm^{-2}}$), *ANT* the anthropogenic heat production, *SH* the sensible heat flux, *LH* the latent heat flux, and *G* the storage flux (positive downward). Within cities, the lower albedo generally results in a slightly higher Q^* [*Christen and Vogt*, 2004]. In addition, the *LH* component is significantly reduced compared to rural areas due to a lower vegetation cover and consequently lower evapotranspiration. In addition, the soil moisture in urban areas is relatively low, because most of the precipitation runs off directly to the wastewater system. Thus, the net radiation is mostly partitioned into the *SH* and *G*. The sensible heat flux increases (in particular during daytime) due to the larger vertical temperature gradient, between the surface and air temperature. Finally, the storage or soil heat flux is larger than in rural areas due to the larger surface area and different building materials.

[8] Additional factors contributing to the UHI magnitude are the anthropogenic heat flux (maximum $\sim 1 \cdot 10^2$ $\mathrm{Wm^{-2}}$ [*Kato and Yamaguchi*, 2005]), surface roughness, or the specific topography of the cities, where buildings are organized in urban canyons. All these factors cause a heat accumulation in the urban areas during the day and a release of stored heat at night, resulting in higher temperature in cities compared to rural areas [*Oke*, 1982]

[9] Enhanced evaporation can lower the air temperature and thus mitigate the UHI and increase the thermal comfort of inhabitants. More evaporation increases *LH* and affects the energy partitioning of *SH* and *G*, such that an *SH* reduction and a decrease in the magnitude of *G* introduce a relative temperature decrease in the urban canyon. Increased evaporation can be achieved by increasing vegetation or the amount of surface water.

[10] Several studies concerning the influence of vegetation on urban temperatures are available. For example, *Huang et al*. [2011] assessed the impact of the size and distribution of vegetation in a city during daytime. On the other hand, studies reporting the effectiveness of water in mitigating the urban heat are relatively scarce. Only a few studies hypothesize water bodies as the strongest cooling element in the city during hot summer days [*Rinner and Hussain*, 2011; *Oláh*, 2012]. However, these studies are mostly from a measurement perspective, either using field observations or remote sensing data and with a strong focus on the daytime. Therefore, the current study focuses on the influence of open water on day- and nighttime urban temperatures and thermal comfort.

[11] Water is commonly used in urban planning as a decorative aspect of public places [*Kleerekoper et al*., 2012]. The cooling effects of water bodies, such as lakes, rivers, or fountains, have been studied and known for quite some time [e.g., *Xu et al*., 2009 and *Sun and Chen*, 2012]. In some cities, water is an inseparable part of everyday life, e.g., for cities on a riverside or next to lakes. For example, *Xu et al*. [2009] used observations to study the influence of a water body on thermal comfort, for very hot days with air temperatures above 35°C. Their results indicate that the water bodies with a surface area larger than $2.10^4\,\mathrm{m^2}$ significantly cool their littoral zones. Concurrently, a modeling study conducted by *Robitu et al*. [2004] showed that small ponds ($4\,\mathrm{m^2}$) have a cooling effect on their surroundings as well. Another study focused on the cooling effect of water-holding pavements; this showed a temperature decrease of several degrees centigrade [*Nakayama and Fujita*, 2010].

[12] The impact of water bodies on urban temperatures has not been completely unraveled [*Steeneveld et al*., 2011]. In addition, a systematic study (i.e., excluding local effect of city specific issues) to the role of the spatial distribution of water bodies has not been performed yet. Most of the studies also focus on either nighttime, when the UHI is strongest, or daytime, when the extreme temperatures in the city may be potentially dangerous to the health of inhabitants.

[13] In this study, a lake with a constant temperature shifts the energy balance partitioning above the lake to cause a decrease in the sensible heat, leading to an increase in latent heat. This limits the heat in the city. On the other hand, with higher evaporation, the air humidity increases as well. Thermal comfort is a combination of many factors, such as, temperature, wind speed, or the relative humidity, radiation, clothing, and metabolism [*Budd*, 2001]. Higher air humidity lowers the thermal comfort and counteracts the effect of evaporation on temperature. The net effect on the thermal comfort of inhabitants is given by superposition of these aspects.

3. Methodology

[14] In this section, the methodology are presented. First, the numerical model (WRF) is described and its settings are explained. Second, a general case description is given with the specific approaches to the sensitivity experiments. Finally, the analysis is shortly explained.

3.1. Model Description

[15] In order to investigate the influence of surface water on urban temperature and thermal comfort, we use the Weather Research and Forecasting (WRF) Model version 3.2.1 with the ARW core [*Skamarock et al*., 2008]. The most important settings of the model are displayed in Table 1. In order to represent the urban canopy in the model, the single layer urban canopy model [*Kusaka et al*., 2001, *Chen et al*., 2011] with adjustments from *Loridan et al*. [2010] is used, which is coupled to the NOAH land surface scheme [*Ek et al*., 2003]. It calculates the momentum and energy exchange between atmosphere and three types of urban facades: roofs, walls, and roads. This model also takes into account the influence of specific geometry of the street canyons and includes the

Table 1. A Summary of the Most Important Model Settings

General Settings	
Time	7 May 2008, 06:00 – 10 May 2008, 18:00 UTC
Grid size	D1: 32 × 32
	D2: 60 × 60
	D3: 100 × 100
Horizontal resolution	D1: 25 × 25 km
	D2: 5 × 5 km
	D3: 1 × 1 km
Vertical resolution	35 eta levels
Initial, boundary conditions	1° × 1° six-hourly NCEP-FNL data
Parameterizations	
Land surface	NOAH
Urban canopy model	Single layer urban canopy model with:
	Default settings for high-intensity residential area
	Anthropogenic heat: 0 Wm^{-2}
Boundary layer	MRF (default)
	MYJ (sensitivity analysis)
Eddy coefficient	Smagorinsky first-order closure
Horizontal diffusion	Sixth-order numerical diffusion, prohibiting up-gradient diffusion
Microphysics	WSM3 simple ice
Longwave radiation	CAM
Shortwave radiation	Dudhia
Convection scheme	Grell-Devenyi
Surface Properties	
Roughness length	Grass: 0.12 m
Albedo	Grass: 0.19
Emissivity	Grass: 0.985
Soil moisture	Grass: 0.27 m^3m^{-3}
	Urban: 0.33 m^3m^{-3}
Soil temperature	Grass and Urban:
	L1: 290.0 K
	L2: 285.5 K
	L3: 284.5 K
	L4: 283.0 K

shadowing from buildings. The single layer urban canopy model is used in this study because the temperature within the city is analyzed during day- and nighttime. In particular, during nighttime, an urban canopy model represents the urban boundary layer better than a slab model, due to the trapping of radiation included in the urban canopy model.

[16] Several versions of this model along with many other urban canopy models are studied in *Grimmond et al*. [2010, 2011]. Their study showed that no urban canopy model performed best for all parts of the energy balance. *Loridan et al*. [2010] and *Wang et al*. [2011] found that within the single layer urban canopy model used in this study, the net radiation is vulnerable to changes in the albedo of the facades and to the urban geometry. In addition, the sensible heat flux is especially sensitive to thermal properties and the thickness of the roof and the geometry of the street canyon (building height and roof width). Finally, the storage heat flux responds largely to changes in the thickness of the facades and again the canyon geometry.

[17] Since this study aims to formulate generally valid conclusions, i.e., not restricted to one particular city or water body, the research uses an idealized case. Hence, it is difficult to validate this case with observations. A brief quality check will be presented in section 4.1. However, WRF is a widely used tool in urban modeling and has been validated for different cities, such as Beijing [*Miao et al*., 2009], New York City [*Holt and Pullen*, 2007], London [*Loridan et al*., 2013], and Taiwan [*Lin et al*., 2008] as summarized in *Chen et al*. [2011].

[18] The model setup contains three nested domains with 32 × 32, 60 × 60, and 100 × 100 grids. The grid length for these domains equals 25, 5, and 1 km respectively. This domain setup is required for the downscaling from the one-degree resolution boundary conditions (1° × 1° six hourly NCEP-FNL data) to 1 km resolution of the smallest domain. In the middle of the third domain, a circular city is created. The simulations use 35 eta levels in the vertical direction with nine levels below 1000 m, and with the lowest model level at ~22 m. In addition, the model spin-up is 24 h.

[19] In order to study the sensitivity to the selected ABL scheme, we repeated our study using two different permutations of the ABL schemes, described in more detail in section 3.5. The nonlocal, Medium-Range forecast scheme (MRF) [*Troen and Mahrt*, 1986] and the local, Mellor-Yamada-Janjic (MYJ) [*Mellor and Yamada*, 1982; *Janjic*, 1990] are used. The simulations with the MYJ scheme generated some rolls-type structures in vertical cross section of potential temperature. The same structures were observed by *Salamanca et al*. [2012] as well, who used a fixed diffusion coefficient to circumvent this model artifact. For this reason, we use the same value of horizontal diffusion; 300 m^2s^{-1}, with the horizontal Smagorinsky first-order closure scheme.

[20] For completeness, our runs use the WSM3 simple ice microphysics scheme [*Hong et al*., 2004], the CAM [*Collins et al*., 2004] longwave radiation scheme, *Dudhia* [1989] for the shortwave radiation, and the Grell-Devenyi convection scheme. Finally, the sixth-order numerical diffusion, prohibiting up-gradient diffusion is used.

3.2. Numerical Setup

[21] An idealized, circular city with monotonous natural surroundings is created in the model environment. In order to ensure a substantial effect in the mesoscale model sensitivity studies, the city has a 50 km diameter; almost 2.10^3 grid cells. This diameter is representative for cities as London, Paris, or Phoenix [*Chow et al*., 2012]. The parameters used in the urban canopy model are the default parameters for a high-intensity residential area as defined by *Chen et al*. [2011]. The only deviation from these default values is that no anthropogenic heat flux is prescribed.

[22] The city is located in Europe (52°N, 7.5°E), relatively far from the sea (not closer than 150 km) in order to prevent the influence of a sea breeze, which is beyond the scope of this paper. For the initialization and boundary conditions, weather conditions from 7–10 May 2008 have been selected. These days were relatively warm (18–25°C) and sunny without clouds over this part of Europe. This was dictated by a high-pressure system with its center located north of the Netherlands (Figure 1). The 10 m wind speed was between 2.5 and 5 ms^{-1} from a southeasterly direction.

[23] The simulation time was 84 h, starting on 7 May 06:00 and ending on 10 May 18:00, 2008. The first 24 h are spin-up time and were not included in the analysis.

[24] In order to exclude local effects of the surrounding rural areas such as orographic effects or the effect of variable land use, the area surrounding the city has been set to grassland with a fixed terrain height of 10 m. The prescribed roughness lengths are 0.33 m for the urban canopy, based

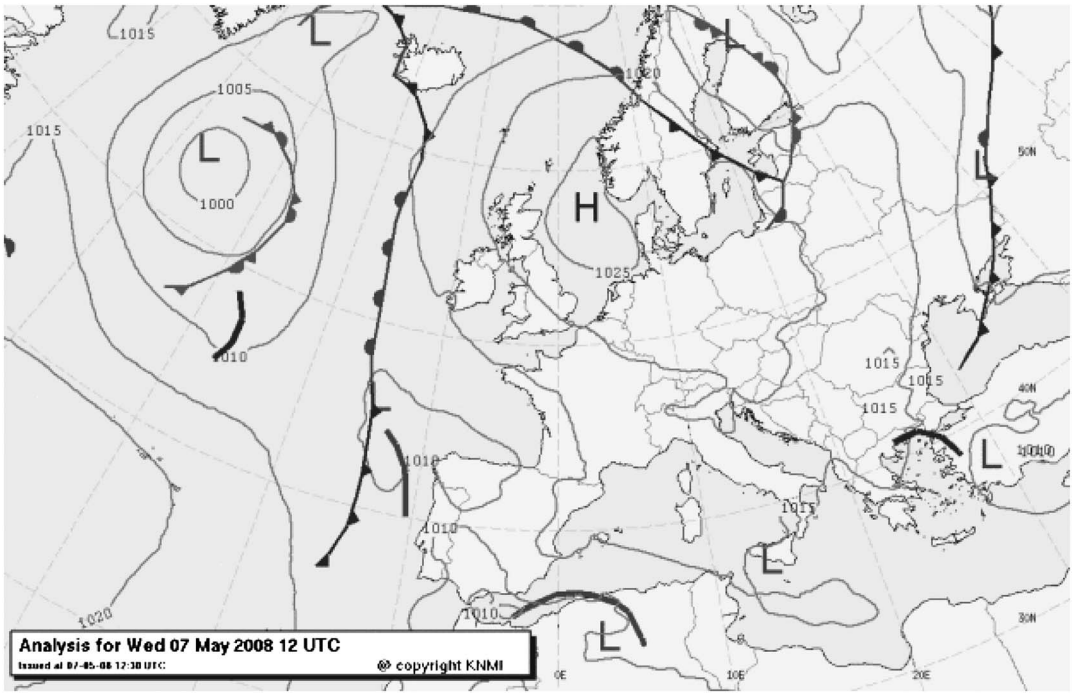

Figure 1. Synoptic situation in Europe on 7 May 2008 at 12 UTC. H and L indicate the center of high- and low-pressure systems, respectively. Semi-circles indicate warm fronts, triangles indicate cold fronts and combined semi-circles and triangles represent the occlusion fronts.

on the building and displacement height, and 0.12 m for grass (with a few shrubs), and in the city the albedo is 0.20 for individual facades (road, roof, and walls) and the grass has an albedo of about 0.19, while the emissivity is set to 0.90 for the roof and wall and 0.95 for the road within the city and 0.985 for grass. In addition, the soil type and initial soil moisture have been modified. These factors can influence the air temperature development and therefore they have been unified all over the domains. As soil type, we selected the most common type in this region (i.e., loam) and the soil moisture was adjusted after a number of consecutive test run for the resulting soil moisture; in this case, 0.27 m^3m^{-3}. Within the city, the soil moisture as provided by NCEP was higher than realistic for a city, i.e., 0.439 m^3m^{-3} for all levels, and the soil temperature was relatively low, i.e., 283 K for all soil levels. As a result, during the simulation, the soil was warming and drying for more than two days before reaching an equilibrium value. To avoid the possible consequences of this spin-up artifact on the air temperature, we have set the equilibrium values of the soil temperature achieved after multiple iterations of the WRF forecast, as initial for all the model runs. The soil temperature is changed to 290 K, 285.5 K, and 284.5 K for the soil surface, first, and second level, respectively. The third soil level is left unchanged, because it does not experience any significant temperature change within the simulated four days. In addition, the soil moisture in the urban area is changed to 0.33 m^3m^{-3} for all levels in an analogue procedure similar to the soil temperature.

[25] Three approaches are used to meet the research objectives. Initially, the different water temperatures are evaluated, secondly, the distribution and surface area of the water over the city is varied, and finally, the study compares two ABL schemes. Two reference runs are performed: one run with the city without any water bodies inside and another with neither a city nor a lake.

3.2.1. Water Temperature

[26] The first sensitivity experiment evaluates the influence of open water bodies on urban temperatures for different lake water temperatures. We hypothesize that colder water has a larger cooling effect and very warm water may even increase the urban temperature. This situation may occur when the air cools to below the water temperature. In order to investigate these possibilities, we prescribe three different lake temperatures, constant in time. For deep, well-mixed lakes or rivers, it is not unrealistic to assume the water temperature stays constant over a period of three days.

[27] In the first case, the lake water temperature is 10°C, which is always lower than the air temperature in the city. The second lake water temperature, 15°C, has been chosen as a typical water temperature for May in western part of Europe. However, that time of the year is when the water temperature changes. Therefore, also the 10°C can be considered realistic for this time of the year. The third lake water temperature is 20°C; this temperature can easily be reached during autumn, when the air temperature is similar to spring, but the water has been heated during summer.

3.2.2. Lake Distribution and Percentage of Surface Water

[28] Additional important factors connected to the influence of a water body on the air temperature are the sizes and distribution of the water masses. Typical percentage of water cover in European cities typically varies between 6% in Berlin and 25% in Amsterdam. During this experiment, the percentage of water in the city varied between 5, 10, and 15% of a total size of the city, with 10% for the default experiment.

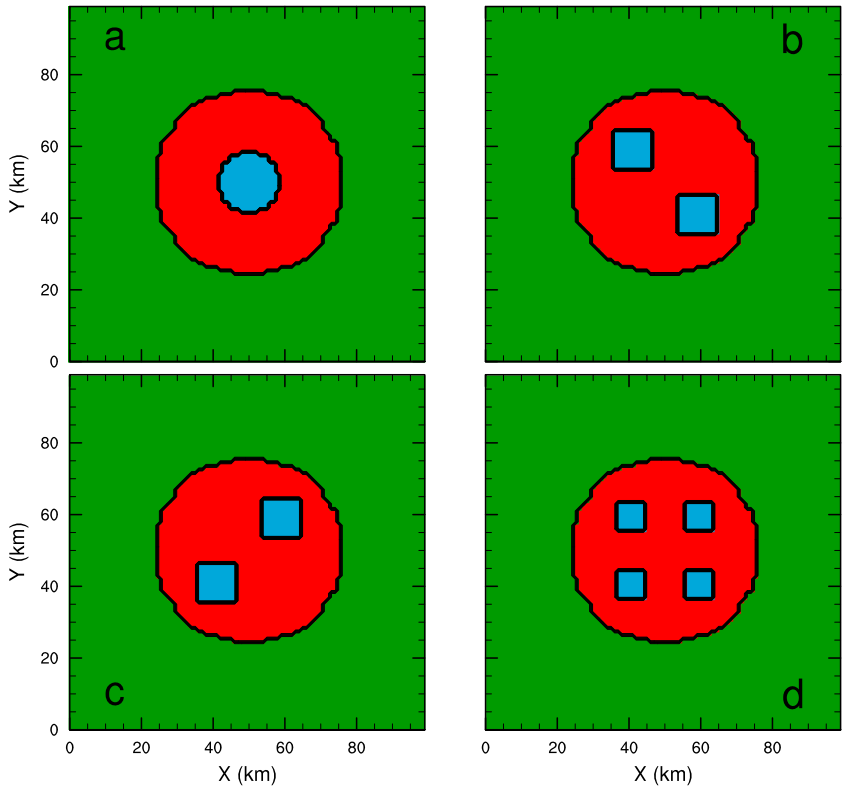

Figure 2. Case setup of different distributions of surface water in the city.

[29] In order to study temperature effects of spatially differently distributed water surfaces for each lake temperature, three percentages of surface water and both ABL parameterization options, four different spatial distributions are analyzed (see Figure 2). First of them is the default lake case; here all water is stored in one big lake in the middle of the city (case A). The second and third cases have two lakes, each on one of the diagonals of the city (cases B and C). Because the temperature effect in an urban area usually occurs downwind from the lakes, the different locations of these lakes in the city should simulate how it will be affected if the wind is from a different direction. These two particular ways of positioning the two lakes are chosen such that one of them represents a case where a large part of the city experiences the influence of the lakes (case C). In the other case, the lakes are behind each other with respect to wind (case B) and therefore the influenced area is expected to be smaller than in the previous case. The last approach shows the influence of four small lakes evenly distributed over the city (case D).

3.2.3. ABL Schemes

[30] The topic we study is a typical ABL phenomenon, and as such it is valuable to quantify the sensitivity of the results to different ABL schemes. Therefore, the results for two different ABL schemes are compared, MYJ and MRF. The MRF scheme is a first-order, nonlocal closure, which means that it accounts for large eddies that effectively transport energy and mass through the ABL. The MYJ scheme is a local scheme that only accounts for vertical transport from neighboring grid cells. The literature indicates that MRF has more skill in representing the heat transfer between surface layer and the ABL than the MYJ scheme and therefore is more advantageous during the day [e.g., *Holtslag and Boville*, 1993]. On the other hand, earlier model evaluations revealed that MRF might overestimate the surface sensible heat flux [e.g., *Steeneveld et al.*, 2008], especially in convective conditions for areas with high surface roughness. In contrast, the MYJ scheme gives a better representation of the ABL during night [e.g., *Willett and Sherwood*, 2012], when MRF overestimates the turbulent transport. MYJ also tends to produce a colder and shallower ABL during the day [*Mellor and Yamada*, 1982].

[31] To simplify the discussion of our model results, we introduce abbreviations for each run composed from the ABL scheme, lake distribution case (described in section 3.2.2), and water temperature. For example, the run with MRF, with one lake covering 10% of the city area with water temperature of 20°C is labeled MRF_A10_20. For the run without lakes and the run without city or lake, we use "MRF_city" and "MRF_nocity," respectively.

3.3. Analysis

[32] This study mostly focuses on the temperature change caused by the introduction of open water in an urban area. Several methods are used to assess the effects of the modifications. First, we use a method that averages the temperature change over the entire city, providing a rough estimate of how the particular case influences the whole city. A second method only assesses the part of the city that is directly influenced by the water bodies, the plume. Then, we compare the average temperature change downwind of the lake, the temperature change on the edge of the lake, and further in the city. In addition, we analyze which areal percentage of the city experiences a substantial change in temperature.

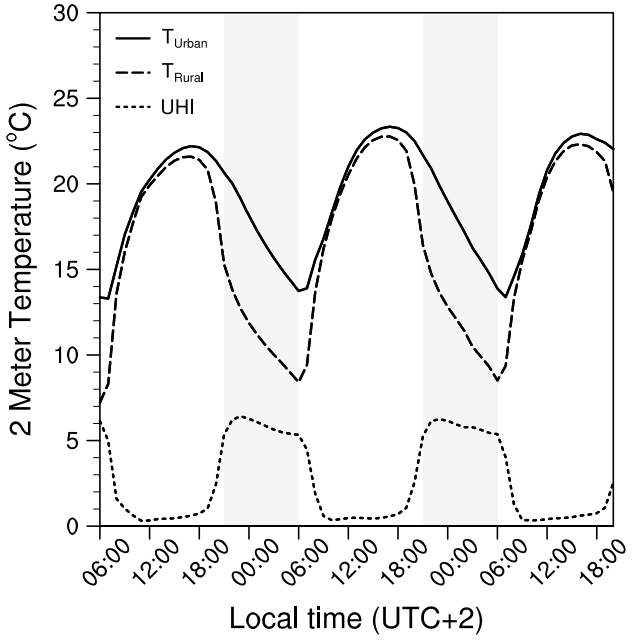

Figure 3. Diurnal variation of temperature in degrees Celsius. Dashed line indicates the temperature at a point in the middle of the domain ($x = 50$, $y = 50$) where no city is simulated, full lines give the same point in the domain in the city simulation, and the dotted line is the difference between these two. Grey panels depict night hours.

[33] In order to investigate the influence on human thermal comfort, the wet bulb globe temperature (*WBGT*) is used, defined as [*Willett and Sherwood*, 2012]:

$$WBGT = 0.567T_a + 0.393e + 3.94, \quad (2)$$

where T_a [°C] is the air temperature and e [hPa] water vapor pressure. This index depends on air temperature and humidity of the air and therefore is well applicable for this case.

4. Results

[34] This section summarizes the results of our model experiments. As a start, we assess the UHI generated by the model and describe the general patterns in the temperature change caused by the introduction of a water body. Subsequently, a detailed description of results connected to different sensitivity analyses is presented. The last paragraph of this section describes the influence of the introduction of the lakes in a city on thermal comfort.

4.1. General Results

[35] First, the magnitude of the UHI generated by the default simulation (MRF_city) is determined. In Figure 3, the UHI is defined as the difference between the 2 m air temperature in the city center and in the rural center (MRF_nocity). Hence, there is no chance that the rural temperature is influenced by the urban plume. It appears that the modeled UHI varies from around 1°C during late morning and early afternoon to values around 6°C in the early night (Figure 3). This seems a realistic UHI, considering findings in earlier observational studies within Europe [e.g., *Hidalgo et al*., 2008, *Steeneveld et al*., 2011]. In addition, the UHI diurnal cycle is similar to the classical behavior for an urban-rural temperature contrast as described by *Oke* [1982].

[36] The order of magnitude of the UHI in the model results for this particular case has been corroborated by analyzing the observed UHI in an urban area closed to the modeled location. As an example, the Ruhrgebied in Germany (including Essen, Bochum, Duisburg, Dusseldorf, etc.) is an urban area of similar size as the city in this study. Two hobby meteorologist urban stations in Bochum in two different environments are used for this, compared to the same rural station (lat: 51.647, lon: 7.199). The first station is located close to an area with very little vegetation and high emissions of anthropogenic heat (lat: 51.477, lon: 7.159). The second station is located close to the center of the city and to a park (lat: 51.486, lon: 7.211). The measurements indicated a UHI of 3°C at 21:00 local time during the first night shown in Figure 3. This value increased during the night until the maximum UHI of 7.8°C was reached at 6:00 local time. In contrary to the measurements of the first station, the second urban measurement station recorded the maximum UHI of 2.7°C at 22:00 local time and decreased slowly to remain around 1.5°C for the remainder of the night. These two stations show the diversity of the UHI within the city. Therefore, it is not possible to correctly compare this idealized case with homogeneous surroundings to real urban

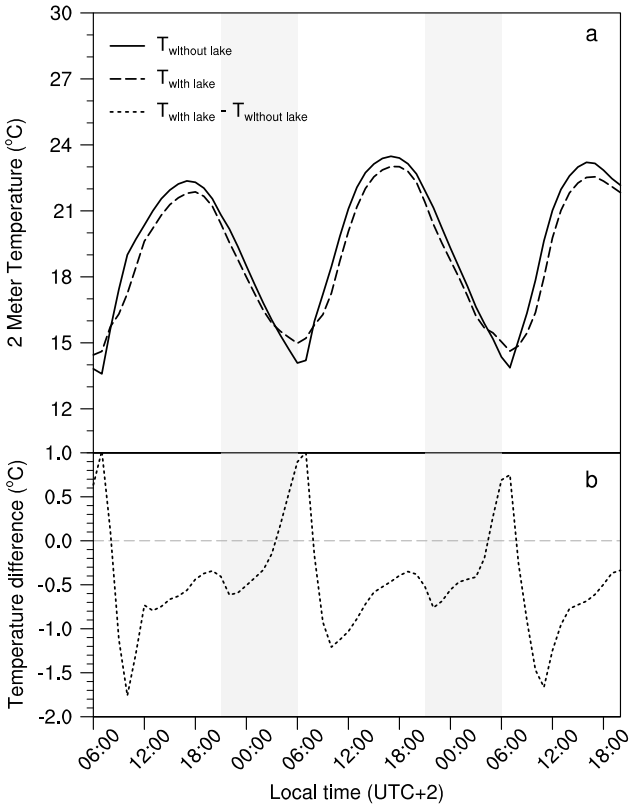

Figure 4. Diurnal variation of (a) temperature in a city without a lake (solid line) and with a lake in the middle of the domain (dashed line) and (b) the temperature difference between the simulation with and without a lake (dotted line), from MRF_A10_15 at a chosen point close to the lake ($x = 40$, $y = 55$). Grey panels depict night hours.

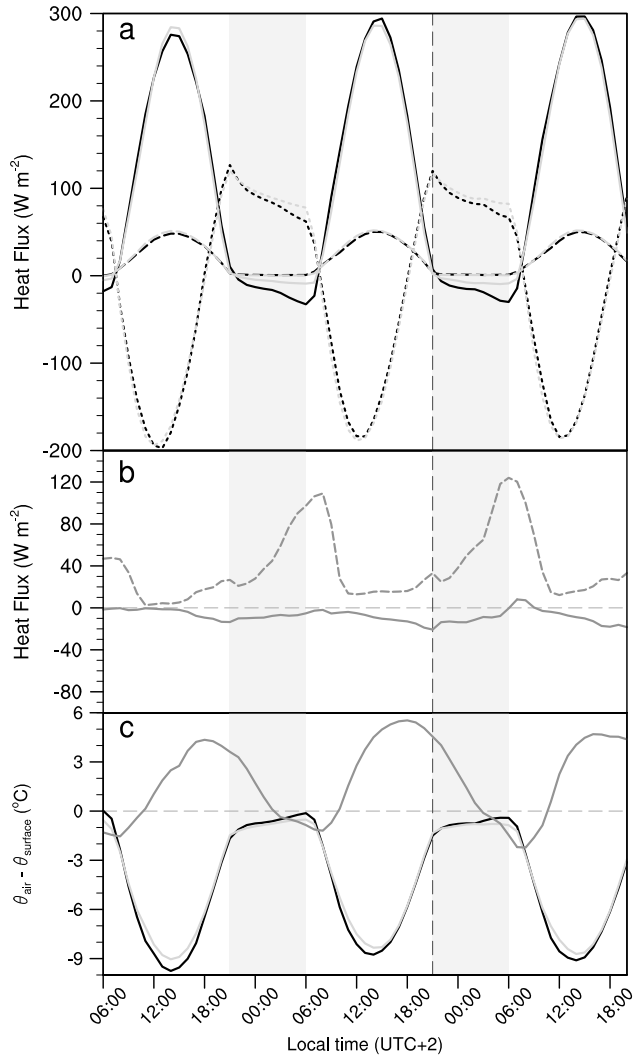

Figure 5. Energy balance components (a), the sensible (solid lines), latent (dashed lines), and storage flux (dotted lines) leeward ($x = 42$, $y = 53$) (black) and windward ($x = 60$, $y = 40$) (light grey) of the lake within the city and (b) the sensible (solid lines) and latent heat flux (dashed lines) over the lake ($x = 50$, $y = 50$) (dark grey). (c) Shows the potential temperature gradient between the temperature at the first model level (22 m) and the surface temperature leeward (black), windward (light grey), and above the lake (dark grey). Vertical black line highlights the situation at 21:00 local time 9 May 2008.

field measurements. However, the model shows UHI results in between these measurements, indicating the correct order of magnitude.

[37] Apart from the temperature effect, the city also affects wind speed and direction. Urban areas have a higher roughness length than the grassland surrounding the city. Therefore, the wind is slowed down and funneled. As a result, we find a difference in wind pattern between the MRF_city run and the MRF_nocity run. The largest difference in the wind speed occurs at night; when the 10 m wind is 2.5 ms^{-1} lower in the city center than in the areas not influenced by the city, and when the air above the city is still unstable or neutral and the air above the rural area is stable. The smallest differences are around noon, when the deviation of the 10 m wind speed in the city center and the rural area is around 0.5 ms^{-1} (not shown). During daytime, the difference in wind speed between rural and urban areas is small because the turbulent mixing is high. At this time, the atmosphere is unstable and turbulence is dominantly produced by buoyancy. This buoyancy is strong enough to mix air parcels with a high momentum toward the surface. The efficiency of the turbulence is approximately similar in the city and over the grassland.

[38] Another aspect that influences the wind speed and direction is the UHI itself. Generally, the warmer air in the city rises and transports in the air from the rural surroundings into the city itself; this effect is called the urban breeze and has been described a number of times before [e.g., *Hidalgo et al.*, 2008]. However, this phenomenon has not been discovered in this modeling study. This is caused by a relatively high background wind speed in this case, which is around 5 ms^{-1} during the day and 2.5 ms^{-1} at night.

[39] In order to streamline the description of the model results, the MRF_A10_15 run is selected to be the default simulation and in each analysis only one of the aspects is varied: the ABL scheme, the water distribution and percentage of water cover, or the water temperature. In order to assess the different water temperatures, we use runs with one lake and the MRF ABL scheme.

4.2. Water Temperature

[40] This section illustrates the influence of different lake water temperatures on the urban air temperature. Therefore, we prescribe the water temperature to constant values of 10, 15, and 20°C.

[41] Figure 4 shows the comparison of the diurnal cycle of temperature and the temperature change caused by the introduction of a lake with 15°C water. The diurnal temperature change has two maxima and two minima. The first temperature change minimum occurs in the early morning (10:00 LT) and represents the time of strongest cooling. This situation takes place when the city temperature rises rapidly, but the water temperature stays constant. In addition, the development of the turbulent ABL starts and allows the relatively cold air originating from the lake to enter the built-up parts. Later during the day, the ABL is deeper, and the cooling by the lake is distributed over a relatively deep layer and therefore the actual cooling is weakened compared to the morning conditions. In addition, during the day, the atmospheric instability downwind of the lake is slightly strengthened by advection of relatively cold air from the lake over a relatively warm surface. This will enhance the vertical turbulent transport of heat away from the surface.

[42] The second minimum occurs around 22:00 LT, i.e., shortly after the sunset, when the city is cooling (most pronounced before sunset of the second day in Figure 4). This minimum is much smaller than the early morning minimum and corresponds to peaks in the components of the energy balance above the lake (negative for *SH*, positive for *LH*; see Figure 5b) and a vanishing *SH* and *LH* for the city (Figure 5a). The peak in the *SH* causes a higher turbulence intensity above the lake.

[43] The explanation for the small secondary peak originates in the turbulent transfer in stable conditions, as over a lake during the day. From basic micrometeorological

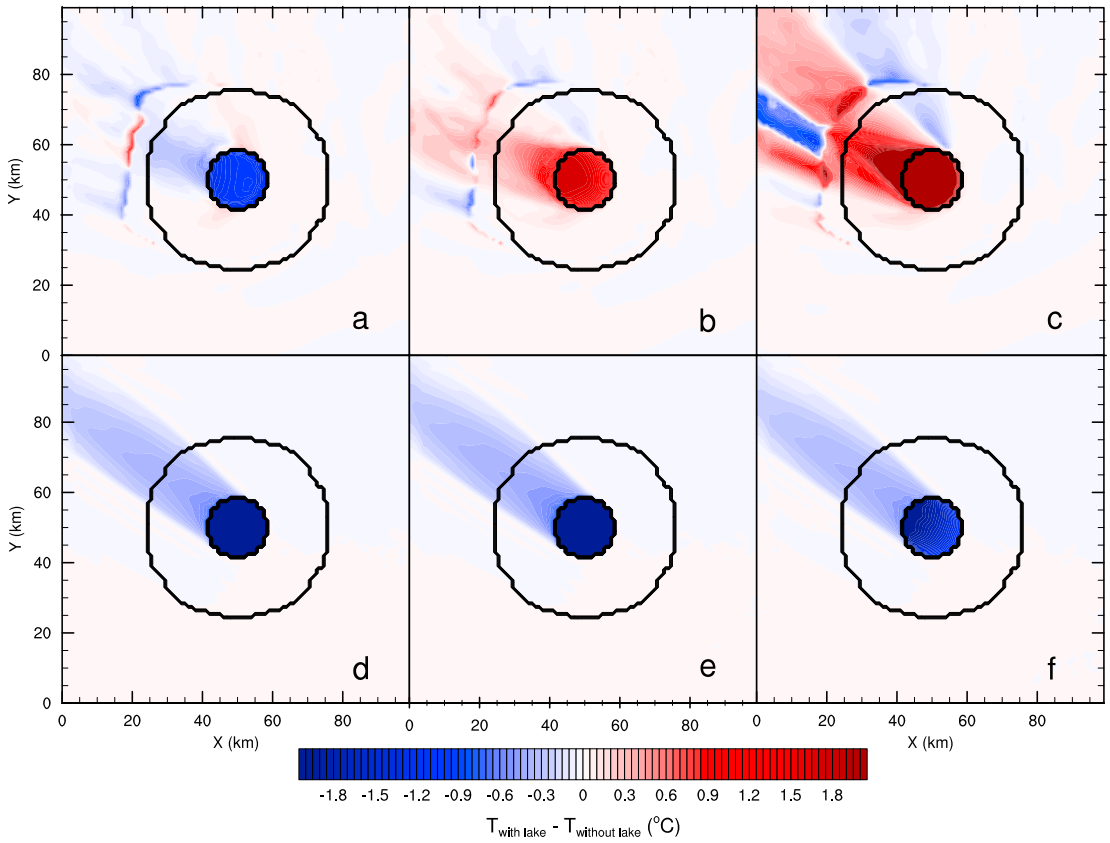

Figure 6. The difference in 2 m temperature between the simulation with and without a lake for different water temperatures, (MRF_A10_10 (10°C a,d), MRF_A10_15 (15°C b,e), and MRF_A10_20 (20°C c,f) for 6:00 and 16:00 local time (UTC +2).

principles, the turbulent heat flux under stable conditions has an optimum with respect to the atmospheric stability [e.g., *Holtslag et al*., 2007]. For small stability an increase in stability will enhance the magnitude of the flux, since the temperature difference between surface and air increased (regime I). For an already very strong stability, an increase in stability will reduce the flux magnitude since the strong stability inhibits the vertical turbulent transfer (regime II).

[44] Hence, in our case, the stability over the lake is very strong during the day (regime II). The stability over the lake decreases before sunset (Figure 5c), which can increase the turbulent intensity. This enhances the *LH* and *SH* magnitudes from the lake, allowing for a temporary faster cooling of the air above the lake. Subsequently, this additionally cooled air is advected downwind and observed as a secondary minimum in the receptor point in Figure 4.

[45] At night, the cooling effect weakens until it vanishes (approximately around 4:00 LT) after which the lake stops acting as a cooling element. This is simply caused by the air temperature being lower than the water temperature. From this time on, the lake starts to warm up its surroundings with the highest intensity around 6:00 LT, when the temperature change is between 0.7 and 1.0°C. The comparison of the simulations with different water temperatures shows that the maximum temperature change is always located on the northwestern coast of the lake (Figures 6 and 7), because the wind direction is southeasterly. The wind is transporting the air from above the lake toward west or northwest (the wind direction slightly changes during the simulation period) and creates a plume of colder or warmer air downwind in the city and further in rural areas. The plume is still present at 22 m as well (Figure 7).

[46] The main difference between the plume at 2 m (Figure 6) and at 22 m (Figure 7) is the temperature difference outside the city during the night. Close to the surface, where the air above grassland is stable, the warm air of the lake (and the city) traveling over the cool air of the rural area can make the air more stably stratified and decrease the temperature in some areas. This effect is strongest with the largest temperature difference, where the lake is 20°C (Figure 6c).

[47] Figure 8 shows the difference in air temperature between the simulations with and without a lake with the distance from the lake in the wind direction. For a water temperature of 10°C, the water body in the city always works as a cooling element. Here, the air temperature is never below the lake water temperature. For a water temperature of 15°C, the situation is already different. During the day, when the air temperature is more than 20°C, the lake works as a cooling element of the city downwind of the lake. During the night, when the air temperature is below 15°C, the influence of the lake changes. Suddenly, the air temperature is lower than the water temperature and therefore the lake warms its surroundings. In this way, the presence of the lake causes an increase in the air temperature.

[48] Figure 8 shows that the lake has a larger influence on its direct surroundings than on the areas further downwind

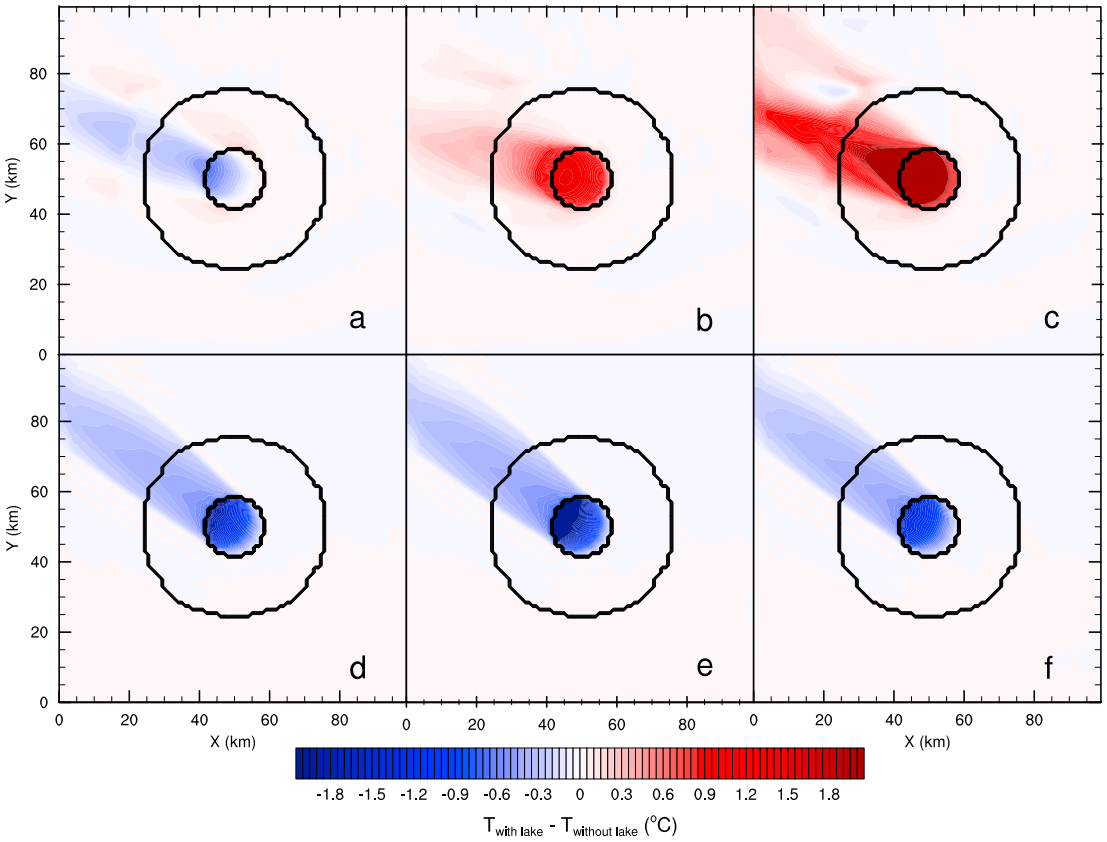

Figure 7. Same as Figure 6 with the temperature difference at 22 m (first model level).

of the lake. The cooling effect of a lake with 15°C temperature can reach 1.5°C or 2°C in areas close to the lake and only 0.5°C or 1°C in the urban location further downwind of the lake (Figure 9b).

[49] The lake with a water temperature of 20°C has a much stronger warming effect during the night than the cooling effect during the day. During the day, the lake cools the city only by about 0.5°C and the shore areas by 1°C (Figure 9c). However, this is not such a significant difference with the 15°C lake. The temperature experiences a much higher influence at night. Close to the lake, the air temperature can be as much as 3.5°C higher than in a case without a lake. This influence again weakens with distance. However, the city location further downwind of the lake experiences air temperatures almost two degrees higher than in a city without lake. This result is consistent with observational findings of Heusinkveld et al. (Spatial variability of the Rotterdam urban heat island as influenced by vegetation cover and building

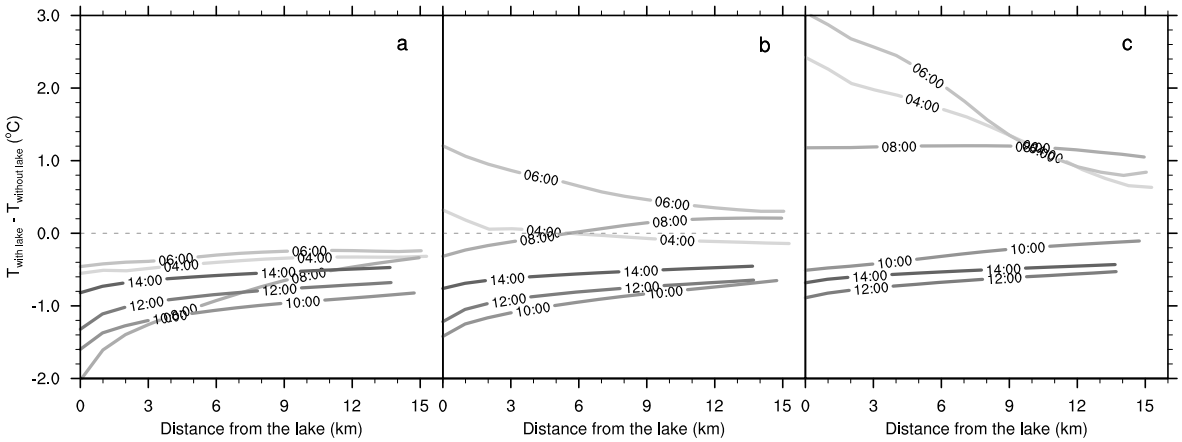

Figure 8. The 2 m temperature difference between the (a) MRF_A10_10, (b) MRF_A10_15, (c) MRF_A10_20, and MRF_city in the urban area with the distance from the lake for several times (local time) during the day. The direction of the line drawn from the lake corresponds with the background wind direction at that time.

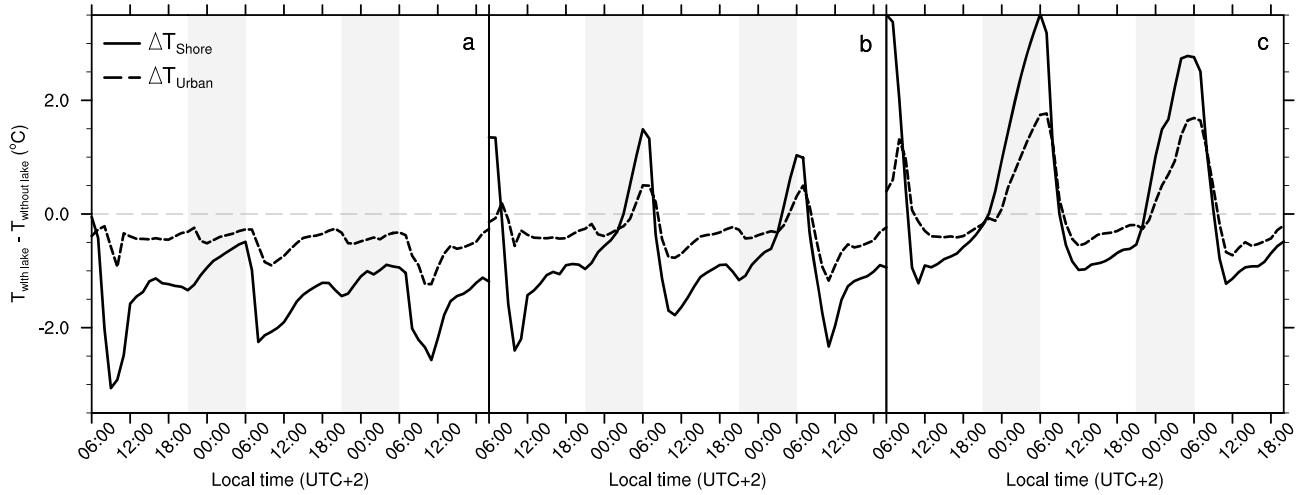

Figure 9. Influence of the lakes of different temperatures on the difference in 2 m temperature at a point close to the lake ($x = 42$, $y = 53$) (solid) and further in the city ($x = 31$, $y = 58$) (dashed). Figure depicts the temperature difference between runs (a) MRF_A10_10, (b) MRF_A10_15, (c) MRF_A10_20, and MRF_city. Grey panels depict night hours.

density, submitted to *Journal of Geophysical Research*, 2013), who found analogue results over the river Meuse in Rotterdam (Netherlands). Also note that the spread in the influence of the lake on the air temperature increases when the lake temperature increases (Figures 8 and 9)

[50] It is important to note that our model simulation does not account for possible heterogeneity in building properties. In reality, building density and building height can be organized such that the flow is obstructed in certain preferential directions. In addition, the urban parameters, prescribed in the model setup, are able to alter the results as well. Consequently, in reality, the flow could follow a different path than shown in Figures 6 and 7. However, our results are inherent to the model setup in which we wish to answer our research question for general conditions.

4.3. Lake Distribution and Percentage of Surface Water

[51] The second analysis concerns the effect of alternative spatial distributions of the water within the city. Figure 10 depicts the percentage of the city that experiences a temperature

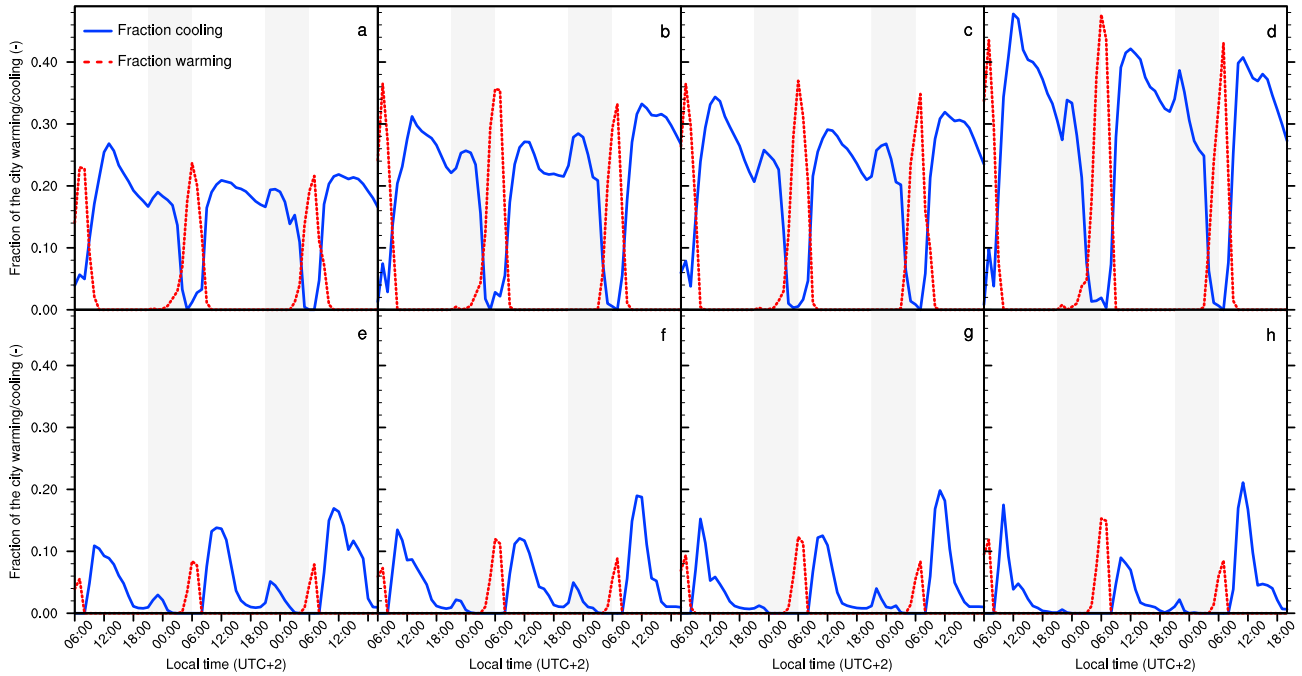

Figure 10. Percentage of the city influenced by the presence of the lake. (a–d) Show the percentage of the city influenced more than 0.1°C and (e–h) percentage of the city influenced more than 0.5°C. Each graph represents one of the model runs for different lake distributions (from left to right MRF_A10_15, MRF_B10_15, MRF_C10_15, and MRF_D10_15). Grey panels depict night hours.

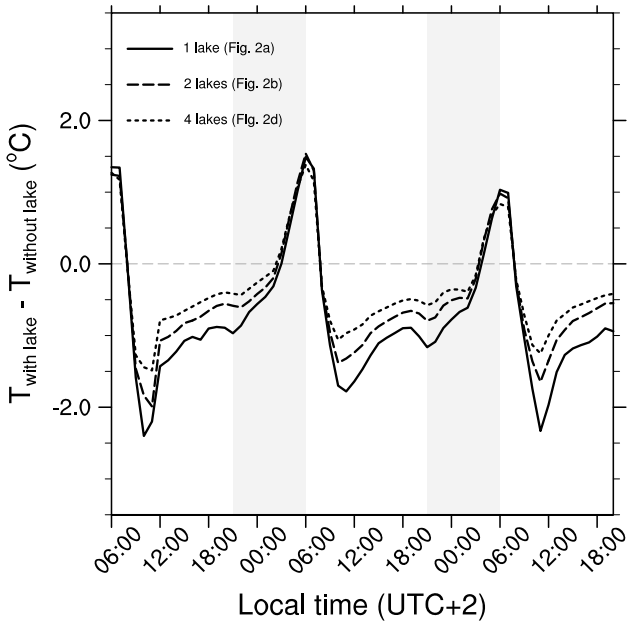

Figure 11. The 2 m temperature difference between the simulations with and without a lake at a point on the coast of lakes of different sizes: MRF_A10_15 ($x = 42$, $y = 53$) (solid line), MRF_B10_15 ($x = 53$, $y = 46$) (dashed line), and MRF_D10_15 ($x = 55$, $y = 44$) (dotted line). Grey panels depict night hours.

change larger than 0.1 and 0.5°C, either warming or cooling. The timing of the transitions from cooling and warming does not change substantially, as well as the approximate times of maximum and minimum temperature changes. However, the percentage of the city influenced by the water body changes significantly. For the simulation with one big lake, 19.3% of the city experiences a temperature change. This percentage can reach up to 26.8%. When the water is distributed more equally over the city, these percentages are significantly higher. For the simulation with four small lakes, an average of 34.3% of the city experiences a significant temperature effect. The largest area of warming of 47.7% is reached at 6:00 LT. At this time, 23.7% of the city area with one lake (MRF_A10_15) experiences this change. The percentage of the city influenced by the temperature change higher than 0.5°C does not show such a large variability within the different cases (bottom panels of Figure 10)

[52] Since the percentage of water in the city was fixed at 10% in the reference case, a higher number of lakes implies that each lake has a smaller size. The area of the water body influences the resulting air temperature change. According to our results, a bigger lake causes stronger cooling than a smaller one (Figure 11). The largest lake cools its closest surroundings up to 2.4°C, while the temperature change at the edge of the lake with four times smaller area only reaches up to 1.4°C.

[53] By examining whether introducing lakes where the water covers ranges from 5 to 15%, it generally appears that a large areal water cover provides a stronger effect on the temperature (Table 2). We can focus on two different situations: the extremes, when the cooling or warming is strongest (maximum warming and maximum cooling), and the average over the city (average cooling, average warming, and average influence). Table 2 shows that the spatial influence increases with the spatial variability of the lakes, as well as with the total water fraction. However, the influence is not linear over the range of water fraction. The temperature effect between 5 and 10% water fraction is more pronounced than between 10 and 15% water fraction. For example, the change between MRF_D5_15 and MRF_D10_15 reaches 9%, while the change between MRF_D10_15 and MRF_D15_15 is only 3.4%. This suggests that a larger spatial water cover does have a nonlinear effect on the air temperature. Therefore, a strategic distribution of a lower amount of water can be more effective than simply adding more surface water.

4.4. Sensitivity to Selected ABL Schemes

[54] As described in section 3.2.3, both ABL schemes cause a different model response. Figure 12 shows that MYJ generates an ABL that is shallower than MRF since the cooling over the lakes is distributed over a smaller layer. We also find that the vertical heat transport at night is strongest with MRF, because the warming is distributed over a deeper layer than with MYJ, which is consistent with results in, e.g., *Garcia-Diez et al*. [2013]. The MRF scheme is a nonlocal scheme and accounts for vertical gradients over the entire ABL. Contrarily, MYJ is a local scheme and only accounts for local gradients and therefore does not spread the warming effect over the complete ABL.

[55] The general results for MRF as described in the previous section are approximately similar for MYJ. The ABL schemes provide the most prominent differences in the extremes. In Figure 13, it appears that the temperature change due to the lake spread over a wider range with MRF than with

Table 2. Percentage of the City Influenced by the Presence of the Lake ($\Delta T_{2m} > 0.1$°C) for Different Amounts of Water and Different Distributions of the Open Water Surfaces in the City[a]

[%]	5% Water				10% Water				15% Water			
Case	A	B	C	D	A	B	C	D	A	B	C	D
Max warming	20.5	30.4	28.6	36	23.7	35.6	36.4	47.7	27.8	40.9	44.3	51.5
Max cooling	20.5	26.8	23.6	34.6	26.8	33.2	34.4	47.7	31	36.4	41.3	47.9
Avg warming	7.1	12	10.5	14	8.5	13.4	13	16.8	10.1	15.1	15.9	16.9
Avg cooling	12.6	16.2	15.1	19.9	17.3	22.4	22.4	29.5	20.1	24.7	27.8	32.2
Avg influence	14.2	19.2	17.6	23.3	19.3	25.9	26.5	34.3	23.4	29.3	32.2	37.8

[a]*Max warming* and *max cooling* show the percentage of the city at the time when the warming and cooling, respectively, are strongest (the peak values in Figure 10). *Avg warming* and *avg cooling* show the average percentage (in time) of the city experiencing warming or cooling (the time averaged percentage in Figure 10). *Avg influence* shows the average percentage of the city experiencing any temperature change (warming and cooling combined) caused by the presence of the water.

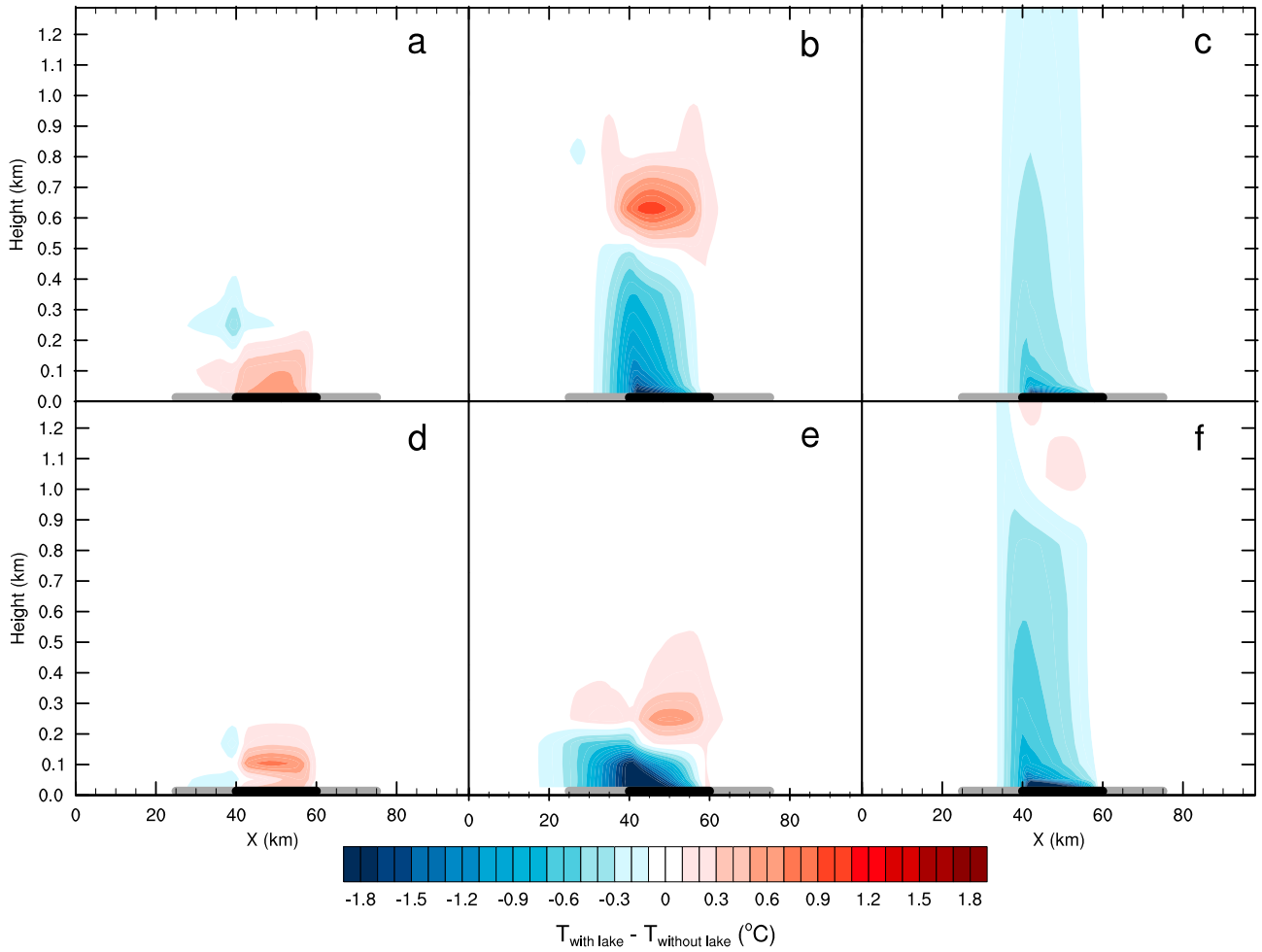

Figure 12. Vertical cross section through the third domain (at $y = 50$) showing the temperature difference between (a–c) MRF_A10_15 and MRF_city , and (d–f) MYJ_A10_15 and MYJ_city for three times during the day: 4:00, 10:00, and 15:00 local time (UTC +2). Grey bars show the position of the city and black the lake.

MYJ. During several hours at night, the average temperature increase is almost 0.5°C and the strongest cooling effect during the day reaches −1°C on average (Figure 13). On the other hand, the number of hours with an extreme cooling effect (air temperature effect higher than 0.5°C) is lower for MRF than for MYJ. With the MYJ scheme, 14 h (out of the simulated 60 h) resulted in a cooling effect higher than 0.5°C, while this is only 11 h with MRF.

[56] Even though the different ABL schemes influence the extremes of the temperature change and the ABL development, the major aspects are consistent, and as such our model findings appear to be robust. Warming and cooling periods have the same length, with exception of two additional hours of warming with MRF compared to MYJ. This difference is caused by the evening transition between the cooling and warming effects of the lake.

4.5. Human Comfort

[57] The difference between the T_a and *WBGT* depends on the water temperature (Figure 14). With a water temperature of 10°C, the humidity in the air always lowers the perceived cooling effect (Figure 14a). For example, in the morning, when the cooling in the air temperature reaches 2.5°C, the perceived cooling is only 0.5°C. This suggests that the humidity causes a discrepancy in the actual and perceived cooling up to more than half (60%). However, such a difference is dominantly visible during the periods of largest temperature change; during the rest of the day, we find that the difference between average air temperature change and average *WBGT* change amounts to 0.5°C.

[58] For a lake with a water temperature of 15°C (Figure 14b), the difference between T_a and *WBGT* depends on the time of the day as well. At night, during the warming episodes, the influence of the air humidity on thermal comfort seems negligible, while during the rest of the day, the difference between the temperature change and *WBGT* change is also around 0.5°C, with extremes reaching 0.8°C difference.

[59] The influence of the air humidity during a period of warming is more pronounced when the warming is relatively strong (Figure 14c). Here, the *WBGT* is lower than the actual temperature and mitigates the warming effect by about 0.8°C. The humidity effect during the cooling period is the same as described above. Generally, the difference between the T_a and *WBGT* change is most pronounced during episodes of the strongest cooling or warming.

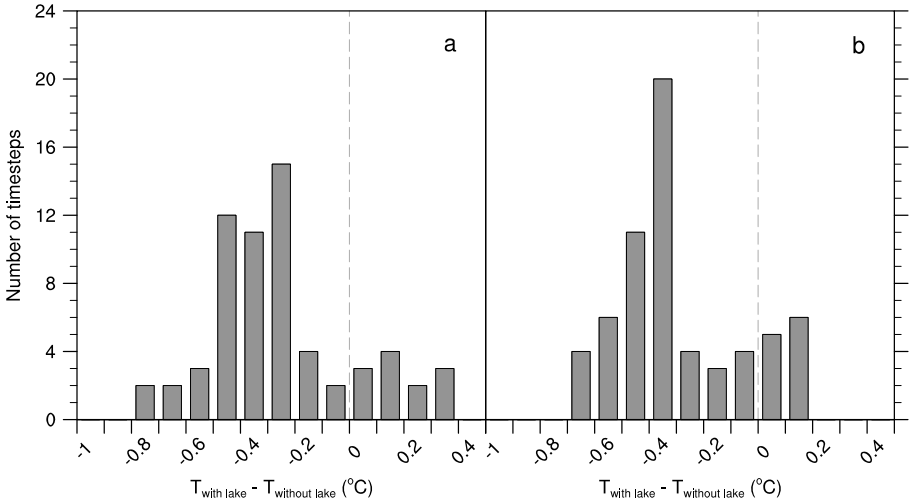

Figure 13. Frequency of time steps of the 2 m temperature difference between simulations with and without a lake, within the plume ($-0.05°C > \Delta T > 0.05°C$), for the two boundary-layer schemes: (a) MRF_A10_15 and (b) MYJ_A10_15 .

5. Discussion

[60] A number of previous studies found that the water bodies in urban areas have a cooling effect on their surroundings [e.g., *Xu et al*., 2009; *Robitu et al*., 2004]. On the contrary, our results indicate that the cooling effect of lakes is only relevant during the daytime, while at night, we find a so far less discussed warming effect. Especially, at night, the thermal comfort is necessary for getting asleep and the critical *WBGT* threshold is lower than during the day. *Moriyama and Matsumoto* [1988] showed that high temperature and humidity inhibit sleep, which subsequently can cause health problems. Our results indicate a warming effect at night, which as such thus counteracts the intended improvement to thermal comfort effect.

[61] Other studies mostly focused on influence of the lakes in their close surroundings [*Kleerekoper et al*., 2012]. However, our study shows that the effect can also influence more distant areas. Colder air originating from the lake is transported by wind and creates a plume of air influenced by the presence of the lake several kilometers long. The size and length of the plume are mostly dependent on the wind. The wind speed during the days of interest was between 2.5 and 5 ms^{-1}, but other wind speeds would lead to different results. Another way to influence the wind over the city is to increase the roughness of the terrain. For example, higher buildings lead to a higher roughness length and slow down the wind over the city. Therefore, various urban parameters will alter the shape of the plume as well.

[62] Furthermore, the size of the lake and distribution of the water over the city play their role. Relatively large lakes also seem to have a relatively strong cooling effect on their surroundings and also longer and colder plume influencing the city downwind. However, several smaller lakes influence

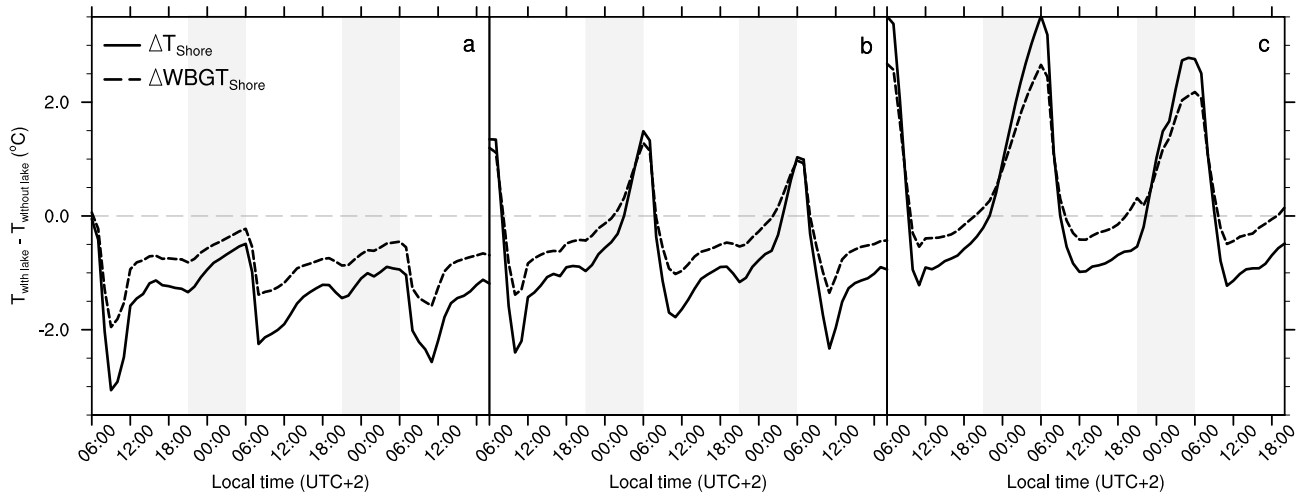

Figure 14. The 2 m temperature (solid lines) and the 2 m WBGT (dashed lines) difference between simulations with and without a lake at a point close to the lake ($x = 42$, $y = 53$). Figure depicts the 2 m temperature difference between (a) MRF_A10_10, (b) MRF_A10_15, and (c) MRF_A10_20 and MRF_city. Grey panels depict night hours.

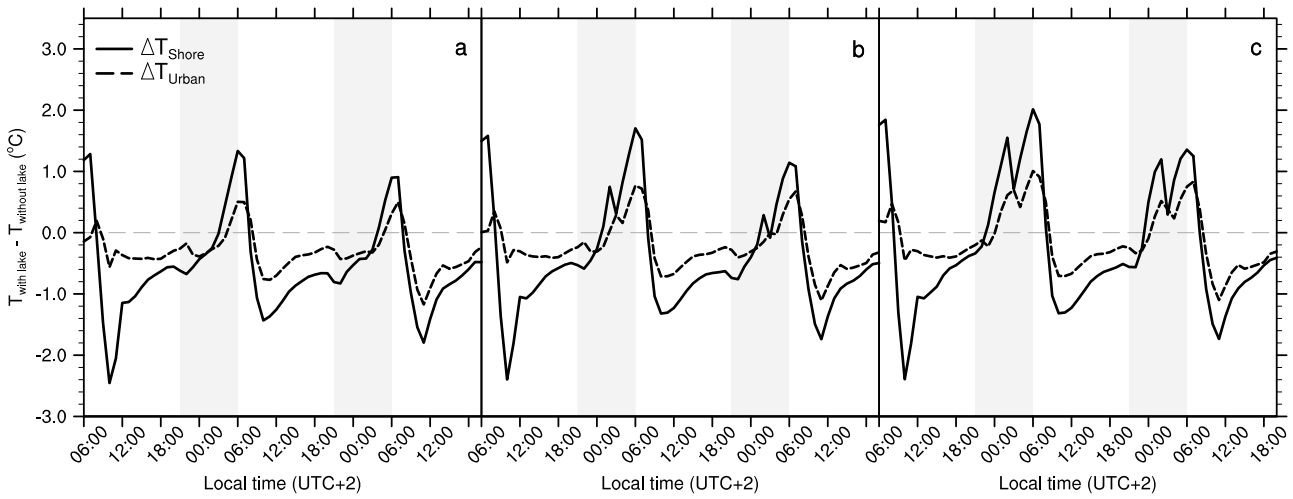

Figure 15. The difference in 2 m temperature for simulations with and without a lake at a point close to the lake ($x = 42$, $y = 53$) (solid) and further in the city ($x = 31$, $y = 58$) (dashed) for (a) constant lake water temperature, (b) a lake water temperature with a diurnal cycle of 2°C, and (c) a diurnal cycle of 4°C. Grey panels depict night hours.

higher percentage of the city. This corresponds to findings of *Sun and Chen* [2012], who also considered influence of the geometry of the water body. With use of large-eddy simulation, they concluded that several smaller regularly shaped water bodies have the most beneficial effect when it comes to lowering extreme temperatures during the day.

[63] Lakes vary in their properties, e.g., well-mixed, deep, large, or small. In this study, a well-mixed deep lake was assumed and therefore a constant water temperature was prescribed. However, during days with high solar radiation and a small amount of mixing within the water, an assumption of a constant water temperature is insufficient [*Kaplan et al*., 2003; *Vercauteren et al*., 2011]. Therefore, Figure 15 shows the diurnal temperature change for a constant lake temperature (Figure 15a) compared to a simulation where the lake water temperature has a diurnal cycle of two degrees varying between 15 and 17°C (Figure 15b). The maximum lake temperature has a delay of 2 h compared to the maximum air temperature. The second simulation has a diurnal cycle of four degrees varying between 15 and 19°C (Figure 15c). These simulations show analogue results for the city temperatures as with a constant lake temperature. Enhancing the diurnal cycle leads to less hours of cooling in the evening and more warming during the night. This amounts to an addition 2 h of warming in the case of a diurnally varying water temperature of 2°C and four additional hours of warming where the water temperature is varied 4°C. These results only enhance the critical point that lakes not only cool during the day but can also be responsible for significant warming in a city. Consequently, in the future, it will be beneficiary to work with an interactive model to simulate the water temperature interactively.

[64] In this study, the *WBGT* is used as an estimate of the influence on thermal comfort. The *WBGT* index only incorporates temperature and humidity. However, this index does not take into account radiation, (mean radiant temperature) the air movement, and therefore the possibility or restriction of sweat evaporation [*Budd*, 2008]. For a more elaborated assessment of human thermal comfort, it would be necessary to use more advanced index, such as Physiological Equivalent Temperature (PET) [*Mayer and Höppe*, 1987], Predicted Mean Votes (PMV) [*Fanger*, 1972], or the universal thermal comfort index (UTCI) [*Jendritzky et al*., 2012]. These methods incorporate various other atmospheric factors such as radiation or wind speed, but also human properties such as age or clothing.

[65] Despite the obvious relation between the urban temperature and the available surface water, a further understanding of the role of lakes in the urban climate needs to be explored. In particular, different influencing factors including the water body area, geometry expressed in the landscape shape index, distance from the city center, and the properties of the surrounding built-up area need to be studied further [*Sun and Chen*, 2012].

6. Conclusion

[66] This study investigates the influence of urban water bodies on the urban air temperature and thermal comfort, using a mesoscale modeling setup of an idealized city and various surface water distributions, area sizes, and temperatures. The air temperature change due to the introduction of a lake depends on the size and number of lakes, distance from the lake, and water temperature. Generally, we find that the influence of the water decreases with the distance from the lake. However, the influence of the lake is still measurable several kilometers downwind of the lake.

[67] Within urban design studies, often the paradigm exists that surface water acts as a cooling element in cities. On the contrary, this study shows that the water temperature (changing per season) mostly dictates the temperature change, overshadowing the cooling due to evaporation. Water with a lower temperature than its surroundings always works as a cooling element and vice versa. This way, the lake works as a buffer of the diurnal cycle of the temperature: cools the environment during the day and warms it at night. A consequence of this finding: when water bodies have reached a higher temperature at the end of the summer season, they can act as nocturnal warming elements and are adverse to thermal comfort.

[68] In addition, the temperature effect of a lake on the city differs for various distributions of the same amount of water over the city. One large lake has a strong effect on its surroundings, while several smaller lakes influence a higher percentage of the city. Moreover, increasing the surface water in a city does not necessarily lead to a linear relationship with the temperature change within a city. Thus, proper weighing of the size and location of the lake can be beneficial to urban planning.

[69] Concerning the sensitivity of our results to the boundary layer schemes, we find that the variance in cooling and warming is similar for the studied MRF and MYJ schemes; however, their results differ in the extreme values. The MRF scheme models a stronger warming and cooling effect of the lake. On the other hand, the MYJ scheme forecasts more hours with very strong cooling (more than 0.5°C difference) than the MRF scheme.

[70] The increased atmospheric humidity caused by evaporation from the introduced lakes decreases the perceived thermal effect of the lake. However, the difference between the air and the WBGT change is substantial and amounts to a maximum of ~0.8°C in some cases. This implies that up to ~60% of the comfort achieved by the cooling effect is cancelled out by the humidity change. These findings can be used in urban planning, where the mitigation of UHI and adverse human thermal comfort becomes more important due to extensive urbanization in the last century.

[71] **Acknowledgments.** We would like to express our appreciation to NCEP-FNL for providing the model input data files for our modeling study, to Rijkswaterstaat for providing the lake temperatures in the Netherlands, and to Weather Underground for the air temperatures in cities and its surroundings. KNMI is acknowledged for providing figure 1. Finally, we would like to thank Thomas Loridan and two anonymous reviewers for their useful suggestions on the manuscript.

References

Budd, G. M. (2001), Assessment of thermal stress-The essentials, *J. Therm. Biol.*, *26*, 371–374.

Budd, G. M. (2008), Wet-bulb globe temperature (WBGT)-its history and its limitations, *J. Sci. Med. Sport*, *11*, 20–32.

Chen, F., et al. (2011), The integrated WRF/urban modelling system: development, evaluation, and applications to urban environmental problems, *Int. J. Climatol.*, *31*, 273–288, doi:10.1002/joc.2158.

Chow, W. T. L., D. Brennan, and A. J. Brazel (2012), Urban Heat Island Research in Phoenix, Arizona: Theoretical Contributions and Policy Applications, *Bull. Am. Meteorol. Soc.*, *93*, 517–530.

Christen, A., and R. Vogt (2004), Energy and radiation balance of a central European city, *Int. J. Climatol.*, *24*, 1395–1421.

Collins, W. D., R. J. Rasch, B. A. Boville, J. J. Hack, J. R. McCaa, D. L. Williamson, J. T. Kiehl (2004), Description of the NCAR community atmosphere model (CAM 3.0).

Dudhia, J. (1989), Numerical study of convection observed during the winter monsoon experiment using a mesoscale two-dimensional model, *J. Atmos. Sci.*, *46*, 3077–3107.

Ek, M. B., K. E. Mitchell, Y. Lin, E. Rogers, P. Grunmann, V. Koren, G. Gayno, J. D. Tarpley (2003), Implementation of Noah land surface model advances in the National Centers for Environmental Prediction operational mesoscale Eta model, *J. Geophys. Res.*, *108*(D22), 8851, doi:10.1029/2002JD003296.

Fanger, P. O. (1972), *Thermal comfort*, McGraw-Hill, New York.

Garcia-Diez, M., J. Fernández, L. Fita, and C. Yagüe (2013), Seasonal dependence of WRF model biases and sensitivity to PBL schemes over Europe, *Q. J. R. Meteorol. Soc.*, *139*, 501–514.

Grimmond, C. S. B., et al. (2010), The International Urban Energy Balance Models Comparison Project: First Results from Phase 1, *J. Appl. Meteorol. Climatol.*, *49*, 1268–1292.

Grimmond, C. S. B., et al. (2011), Initial results from Phase 2 of the international urban energy balance model comparison, *Int. J. Climatol.*, *31*, 244–272, doi:10.1002/joc.2227.

Hidalgo, J., V. Masson, and G. Pigeon (2008), Urban-breeze circulation during CAPITOUL experiment: numerical simulation, *Meteorol. Atmos. Phys.*, *102*, 243–262.

Holt, T. J., and J. Pullen (2007), Urban Canopy Modeling of the New York City Metropolitan Area: A Comparison and Validation of Single- and Multilayer Parameterizations, *Mon. Weather Rev.*, *135*, 1906–1930.

Holtslag, A. A. M., and B. A. Boville (1993), Local versus nonlocal boundary-layer diffusion in a global climate model, *J. Clim.*, *6*, 1825–1842.

Holtslag, A. A. M., G. J. Steeneveld, and B. J. H. van de Wiel (2007), Role of land surface temperature feedback on model performance for stable boundary layers, *Boundary Layer Meteorol.*, *125*, 361–376.

Hong, S. Y., J. Dudhia, and S. H. Chen (2004), A Revised Approach to Ice Microphysical Processes for the Bulk Parameterization of Clouds and Precipitation, *Mon. Weather Rev.*, *132*, 103–120.

Huang, H. Y., S. A. Margulis, C. R. Chu, and H. C. Tsai (2011), Investigation of the impacts of vegetation distribution and evaporative cooling on synthetic urban daytime climate using a coupled LES-LSM model, *Hydrol. Processes*, *25*, 1574–1586.

Janjic, Z. I. (1990), The step-mountain coordinate: Physical package, *Mon. Weather Rev.*, *118*, 1429–1443.

Jendritzky, G., R. De Dear, and G. Havenith (2012), UTCI--why another thermal index?, *Int. J. Biometeorol.*, *56*, 421–428.

Kaplan, D. M., J. L. Largier, S. Navarrete, R. Guinez, and J. C. Castilla (2003), Large diurnal temperature fluctuations in the nearshore water column, *Estuarine Coastal Shelf Sci.*, *57*, 385–398.

Kato, S., and Y. Yamaguchi (2005), Analysis of urban heat-island effect using ASTER and ETM+Data: Separation of anthropogenic heat discharge and natural heat radiation from sensible heat flux, *Remote Sens. Environ.*, *99*, 44–54.

Kleerekoper, L., M. van Escha, and T. B. Salcedob (2012), How to make a city climate-proof, addressing the urban heat island effect, *Resour. Conserv. Recycl.*, *64*, 30–38.

Kusaka, H., H. Kondo, Y. Kikegawa, and F. Kimura (2001), A simple single-layer urban canopy model for atmospheric models: Comparison with multi-layer and slab models, *Boundary Layer Meteorol.*, *101*, 329–358.

Lin, C. Y., F. Chen, J. C. Huang, W. C. Chen, Y. A. Liou, W. A. Chen, and S. C. Liu (2008), Urban heat island effect and its impact on boundary layer development and land–sea circulation over northern Taiwan, *Atmos. Environ.*, *42*, 5635–5649.

Loridan, T., C. S. B. Grimmond, S. Grossman-Clarke, F. Chen, M. Tewari, K. Manning, A. Martilli, H. Kusaka, and M. Best (2010), Trade-offs and responsiveness of the single-layer urban canopy parameterization in WRF: an offline evaluation using the MOSCEM optimization algorithm and field observations, *Q. J. R. Meteorol. Soc.*, *136*, 997–1,019, doi:10.1002/qj.614.

Loridan, T., F. Lindberg, O. Jorba, S. Kotthaus, S. Grossman-Clarke, and C. S. B. Grimmond (2013), High resolution simulation of the variability of surface energy balance fluxes across central London with urban zones for energy partitioning, *Boundary Layer Meteorol.*, *147*, 493–523, doi:10.1007/s10546-013-9797-y.

Mayer, H., and P. Höppe (1987), Thermal comfort of man in different urban environments, *Theor. Appl. Climatol.*, *38*, 43–49.

McCarthy, M. P., M. J. Best, R. A. Betts (2010), Climate change in cities due to global warming and urban effects, *Geophys. Res. Lett.*, *37*, L09705, doi:10.1029/2010GL042845.

Mellor, G. L., and T. Yamada (1982), Development of a turbulence closure model for geophysical fluid problems, *Rev. Geophys.*, *20*, 851–875.

Miao, S., F. Chen, M. A. LeMone, M. Tewari, Q. Li, and Y. Wang (2009), An Observational and Modeling Study of Characteristics of Urban Heat Island and Boundary Layer Structures in Beijing, *J. Appl. Meteorol. Climatol.*, *48*, 484–501.

Moriyama, M., and M. Matsumoto (1988), Control of urban night temperature in semitropical regions during summer, *Energy Build.*, *11*, 213–219.

Nakayama, T., and T. Fujita (2010), Cooling effect of water-holding pavements made of new materials on water and heat budgets in urban areas, *Landscape Urban Plann.*, *96*, 57–67.

Oke, T. R. (1982), The energetic basis of the urban heat island, *Q. J. R. Meteorol. Soc.*, *108*, 1–24.

Oláh, A. B. (2012), The possibilities of decreasing urban heat island, *Appl. Ecol. Environ. Res.*, *10*, 173–183.

Patz, J. A., D. Campbell-Lendrum, T. Holloway, and J. A. Foley (2005), Impact of regional climate change on human health, *Nature*, *438*, 310–317.

Peng, R. D., J. F. Bobb, C. Tebaldi, L. McDaniel, M. L. Bell, and F. Dominici (2011), Toward a Quantitative Estimate of Future Heat Wave Mortality under Global Climate Change, *Environ. Health Perspect.*, *119*, 701–706.

Rinner, C., and M. Hussain (2011), Toronto's Urban Heat Island – Exploring the Relationship between Land Use and Surface Temperature, *Remote Sens.*, *3*, 1251–1265.

Robitu, M., C. Inard, M. Musy, and D. Groleau (2004), Energy balance study of water ponds and its influence on building energy consumption, *Build. Serv. Eng. Res. Technol.*, *25*, 171–182.

Salamanca, F., A. Martilli, and C. Yagüe (2012), A numerical study of the Urban Heat Island over Madrid during DESIREX (2008) campaign with WRF and evaluation of simple mitigation strategies, *Int. J. Climatol.*, *32*, 2372–2386.

Skamarock, W. C., J. B. Klemp, J. Dudhia, D. O. Gill, D. M. Barker, M. G. Duda, X. Y. Huang, W. Wang, W. G. Powers (2008), A Description of the Advanced Research WRF Version 3, NCAR technical note; Boulder, USA.

Steeneveld, G. J., T. Mauritsen, G. Svensson, E. I. F. De Bruijn, J. Vilà-Guerau de Arellano, and A. A. M. Holtslag (2008), Evaluation of Limited-Area Models for the Representation of the Diurnal Cycle and Contrasting Nights in CASES-99, *J. Appl. Meteorol. Climatol.*, *47*, 869–887.

Steeneveld, G. J., S. Koopmans, B. G. Heusinkveld, L. W. A. van Hove, A. A. M. Holtslag (2011), Quantifying urban heat island effects and human comfort for cities of variable size and urban morphology in Netherlands, *J. Geophys. Res.*, *116*, D20129, doi:10.1029/2011JD015988.

Stewart, I. D., and T. R. Oke (2012), Local Climate Zones for Urban Temperature Studies, *Bull. Am. Meteorol. Soc.*, *93*, 1879–1900.

Sun, R., and L. Chen (2012), How can urban bodies be designed for climate adaptation?, *Landscape Urban Plann.*, *105*, 27–33.

Tan, J., Y. Zheng, X. Tang, C. Guo, L. Li, G. Song, X. Zhen, D. Yuan, A. J. Kalkstein, and F. Li (2010), The urban heat island and its impact on heat waves and human health in Shanghai, *Int. J. Biometeorol.*, *54*, 75–84.

Tomlinson, C. J., L. Chapman, J. E. Thornes, and C. J. Baker (2011), Including the urban heat island in spatial heat health risk assessment strategies: a case study for Birmingham, UK, *Int. J. Health Geographics*, *10*, 42.

Troen, I. B., and L. Mahrt (1986), A simple model of the atmospheric boundary layer; sensitivity to surface evaporation, *Boundary Layer Meteorol.*, *37*, 129–148.

United Nations (2005), World Urbanisation Prospects: The 2005 Revision, United Nations, DESA, Population Division, online available: http://www.un.org/esa/population/publications/WUP2005/2005WUPHighlights_Exec_Sum.pdf.

Vandentorren, S., P. Bretin, A. Zeghnoun, L. Mandereau-Bruno, A. Croisier, C. Cochet, J. Riberon, I. Siberan, B. Declercq, and M. Ledrans (2006), August 2003 heat wave in France: risk factors for death of elderly people living at home, *Eur. J. Public Health*, *16*, 583–591.

Vercauteren, N., H. Huwald, E. Bou-Zeid, J. S. Selker, U. Lemmin, M. B. Parlange, and I. Lunati (2011), Evolution of superficial lake water temperature profile under diurnal radiative forcing, *Water Resour. Res.*, *47*, W09522, doi:10.1029/2011WR010529.

Wang, Z.-H., E. Bou-Zeid, A. Siu Kui, and J. A. Smith (2011), Analyzing the Sensitivity of WRF's Single-Layer Urban Canopy Model to Parameter Uncertainty Using Advanced Monte Carlo Simulation, *J. Appl. Meteorol. Climatol.*, *50*, 1795–1814.

Willett, K. M., and S. Sherwood (2012), Exceedance of heat index thresholds for 15 regions under a warming climate using the wet-bulb globe temperature, *Int. J. Climatol.*, *32*, 161–177.

Xu, J., Q. Wei, X. Huang, X. Zhu, and G. Li (2009), Evaluation of human thermal comfort near urban water body during summer, *Build. Environ.*, *45*, 1072–1080.